Phonon transport simulations in low-dimensional, disordered graphene nanoribbons

Neophytos Neophytou
School of Engineering,
University of Warwick,
Coventry, CV4 7AL, UK
N.Neophytou@warwick.ac.uk

Hossein Karamitaheri
Department of Electrical Engineering,
University of Kashan,
Kashan 87317-51167, Iran

***Abstract*— In this work we investigate phonon transport in low-dimensional, disordered armchair graphene nanoribbons (GNRs). We use the non-equilibrium Green's function (NEGF) simulation technique and the force constant method. We focus on how different parts of the phonon spectrum are influenced by geometrical confinement and line edge roughness. In the ballistic case, phonons throughout the entire phonon energy spectrum contribute to thermal transport. With the introduction of line edge roughness, the phonon transmission is reduced, but quantitatively and qualitatively in different ways throughout the energy spectrum. We identify how each region of the spectrum reacts to low-dimensionality and disorder, and elaborate on how phonon transport is affected by that. We explain how and when phonons in different energies within the spectrum flow either ballistically, diffusively, or become localized depending on the channel geometry.**

Keywords*— *theory; simulation; phonon transport; graphene nanoribbons; low-dimensionality

I. INTRODUCTION

Graphene nanoribbons (GNRs) are one-dimensional structures that have attracted significant attention, both for fundamental research as well as for technological applications [1-9]. Ultra-narrow GNRs have been shown to retain at some degree the remarkable thermal properties of graphene. However, the presence of edges can determine its heat transport properties [7, 10-12]. Several works have shown that the transport properties of low-dimensional systems are significantly degraded by the introduction of scattering centers and localized states [7, 9, 10, 13-15]. Carbon related materials such as graphene, nanotubes, and GNRs can have huge thermal conductivities in their pristine form, reaching values as high as of 3080-5150 W/m K at room temperature [2]. Even a small degree of disorder, however, can drastically degrade this superior thermal conductivity. For example, two orders of magnitude reduction in thermal conductivity has been reported for roughened GNRs, but also for several other low-dimensional materials. This significantly improves the thermoelectric properties of such materials, and thus, it creates interest from technological point of view as well [9, 16, 17]. The phonon spectrum of ultra-narrow GNRs and 1D-dimensional channels in general, however, consists of various phonon modes and polarizations, which react differently in the presence of disorder (e.g. line edge roughness) and exhibit different mean-free-paths (MFPs) and localization lengths (LL). A study on how line edge disorder in 1D GNR channels affects phonon modes of different frequencies and wavevectors in the entire phonon spectrum will be extremely helpful in providing insight in thermal transport at low-dimensions.

In this work we theoretically investigate the effect of line edge roughness and confinement in phonon transport in ultra-narrow GNRs for the modes in the entire energy spectrum independently. The basic conclusions of this study can be applied generically to all 1D systems. Four distinct behaviors within the phonon spectrum in the presence of disorder are identified: i) the low-energy, low-wavevector acoustic branches are affected the least by edge disorder; ii) energy regions that consist of a dense population of relatively 'flat' phonon modes (including the optical branches) are also not significantly affected; iii) 'quasi-acoustic' bands that lie within the intermediate region of the spectrum are strongly affected by disorder; iv) the strongest reduction in phonon transmission is observed in energy regions that are composed of a small density of phonon modes, in which case roughness can introduce transport gaps and band mismatch, and drive transport into the localization regime.

II. METHODS

We employ the NEGF method, which can take into account the exact geometry of the roughness without any underlying assumptions, while we describe the phonon spectrum atomistically using force constants. The phonon dispersion can be computed by solving the following eigenvalue problem:

$$\left[D + \sum_{l} D_l \exp\left(i\vec{q}.\Delta\vec{R} \right) \right] \psi(\vec{q}) = \omega^2 \left(\vec{q} \right) \psi(\vec{q}) \quad (1)$$

where D_l is the dynamical matrix representing the interaction between the unit cell and its neighboring cells spaced by $\Delta\vec{R}$, and $\psi(\vec{q})$ is the phonon mode eigenfunction at wavevector $\vec{q}$.

978-1-4673-8156-7/15/$31.00 ©2015 IEEE

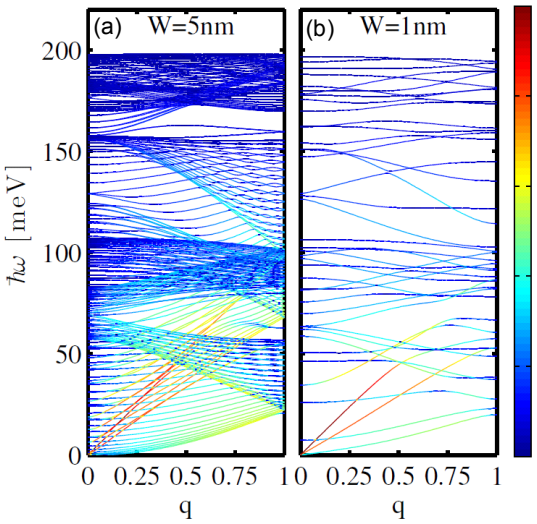

Fig. 1. Phonon dispersions for (a) W=5nm, (b) W=1nm wide GNRs. As the width is decreased, the number of phonon modes is also reduced. The colormap shows the contribution of each phonon state to the total thermal conductance (red: largest contribution, blue: smallest contribution).

The FCM is coupled to NEGF for the calculation of the coherent phonon transmission function in the GNR. The system geometry consists of two semi-infinite contacts made of pristine GNRs, surrounding the channel in which we introduce line edge roughness. The thermal conductance can then be calculated in the framework of the Landauer formalism as:

$$K_1 = \frac{1}{2\pi\hbar}\int_0^\infty T_{\mathrm{ph}}(\omega)\hbar\omega\left(\frac{\partial n(\omega)}{\partial T}\right)d(\hbar\omega) \qquad (2)$$

where $n(\omega)$ is the Bose-Einstein distribution, T_{ph} is the phonon transmission function, and T is the temperature. In this work we consider room temperature T=300K. At room temperature and under ballistic conditions the function inside the integral spans the entire energy spectrum [18, 19], which allows phonons of all energies to contribute to the thermal conductance.

III. The Influnce of Confinement

Figures 1a and 1b show the dispersion relations for GNR channels of widths W=5nm and W=1nm, respectively. The W=1nm case resembles a purely 1D channel, whereas at a width of W=5nm the dispersion diverts towards 2D (although the dispersions in both cases are 1D). These two sizes are computationally manageable, and comparison between their transport properties allows comparison between 1D and less confined, 'towards 2D', phonon transport. The colormap in Fig. 1 shows the contribution of each phonon state to the ballistic thermal conductance at T=300K. To analyze the observed features of the GNR phonon dispersions, we first discuss the graphene phonon dispersion. In graphene, there are 6 phonon modes, 3 acoustic and 3 optical modes [20]. The highest frequency acoustic mode is the longitudinal acoustic (LA) mode, the next one is the in-plane transverse acoustic mode (TA) and lowest frequency mode is the out-of plane

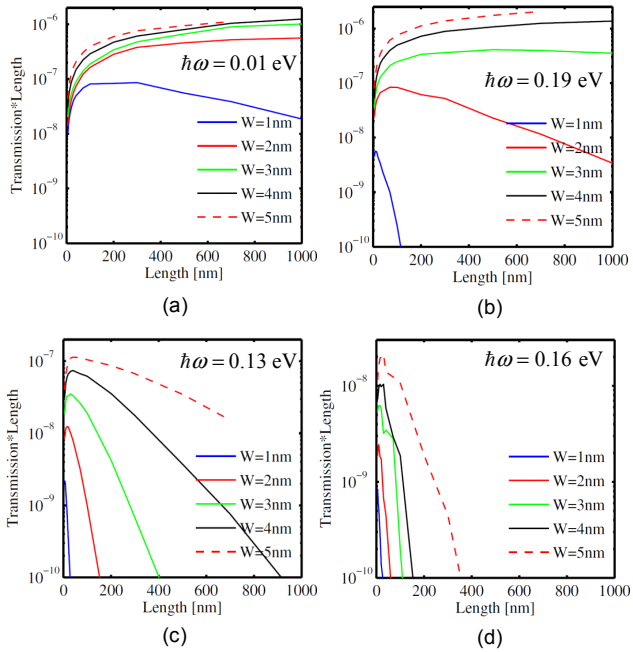

Fig. 2. The phonon transmission times the channel length (T_{ph}×L) versus channel length for rough nanoribbons at energies (a) E=0.01eV, which correspond to the acoustic branches, (b) E=0.19eV, which corresponds to the optical branches, (c) E=0.13eV, and (d) E=0.16eV. In each sub-figure, results for channels of width W=5nm (red-dashed lines) down to W=1nm (blue lines) are shown.

acoustic mode (ZA). The latter is recently shown to make the largest contribution to the thermal conductivity of graphene [21]. The highest frequency optical mode is the longitudinal optical (LO), followed by the in-plane transverse optical (TO), and the lowest is the out-of-plane optical (ZO) [22]. The LA mode of the GNRs shown in Fig. 1 is the corresponding LA mode of graphene with group velocity v_s=19.8 km/s. The LA and TA modes are linear at low frequencies, and extend up to E~0.16eV and E~0.14eV, respectively. The ZA mode is quadratic for low frequencies and extends up to E~0.07eV. At the higher part of their energy region, the acoustic modes become relatively 'flat'. The ZO modes extend from E~0.7eV-0.11eV, whereas the LO and TO modes are located at higher energies, from E~0.16eV-0.2eV. The relatively 'flat' mode regions around energies E~0.07eV-0.11eV consist of ZO modes, in addition to the dispersive LA and TA modes. The less dispersive modes located from E~0.11eV-0.16eV are the 'flat' parts of the LA and TA modes.

Three main changes on the phonon bandstructure can be observed as the width is reduced, i.e. comparing Fig. 1a with Fig. 1b: i) The optical and 'quasi-acoustic' modes (folded acoustic branches of the host material) show strong confinement dependence. The number of modes depends on the number of atoms within the unit cell. As the width is reduced, the number of modes in these regions is also reduced. ii) The number of acoustic modes remains intact, and they carry a much larger portion of the heat (as indicated by their red coloring in Fig. 1a and 1b), especially in the case of the narrower GNR. iii) Small bandgaps appear in some regions in the bandstructure, especially in regions around the interface between the 'flat' optical modes and the more dispersive

'quasi-acoustic' modes (primarily around E=0.16 eV, and secondly around E=0.11 eV, and E=0.07 eV). Large regions in the phononic (E,q) space, especially in the 'quasi-acoustic' band regions, become 'empty' of modes (sparse) where for rather extensive energy and momentum intervals no phonon states exist.

IV. The Influence of Line-Edge-Roughness

Next, we then investigate phonon transport in these low-dimensional GNRs in the presence of disorder. At such small ribbon widths with rough edges, the edge-phonon scattering is the dominant scattering mechanism [15]. For this, we simulate rough GNR channels of width W=5nm (relatively wide) down to W=1nm (purely 1D), and examine the phonon transmission across the phonon energy spectrum as the length of the GNR increases (i.e. as the effective disorder increases). We construct the line edge roughness (LER) geometry by adding/subtracting carbon atoms from the edges of the pristine GNR according to the exponential autocorrelation function.

Since each phonon mode responds differently to disorder, it is essential to investigate the regions of operation of the different modes, and identify the ones that contribute to the semi-ballistic behavior. To illustrate the distinctly different behavior of the various phonon modes in the presence of line edge roughness, Fig. 2 shows the product of the transmission times the length of the channel (T_{ph}×L) versus channel length L at certain phonon frequencies as a function of the channel length L. In the case of ballistic transport, the T_{ph}×L product increases linearly. In the case of diffusive transport it remains constant. In the case of super-diffusive transport the product reduces with length [23], and for localized transport, the product drops exponentially. We focus on four different phonon categories, and pick a specific phonon energy within the energy region of these categories. These are: i) acoustic phonons (E=0.01eV) shown in Fig. 2a, ii) optical, 'flat' dispersion phonons (E=0.19eV) shown in Fig. 2b, iii) 'quasi-acoustic', dispersive phonon modes (E=0.13eV) shown in Fig. 2c, and iv) regions of very low mode densities, in which confinement can even result in narrow bandgaps (E=0.16eV) shown in Fig. 2d. In each figure we consider GNRs of widths W=5 nm (red-dashed lines) down to W=1 nm (blue lines).

From Fig. 2a, it can be seen that for the wider GNR channels, the acoustic modes are ballistic, or semi-ballistic, even for channel widths W=3nm and lengths up to L=1μm. In the ultra-narrow W=1nm GNRs (blue line in Fig. 2a), the acoustic modes reach the diffusive regime at around lengths of L~200nm, and get into the localized regime for lengths larger than L~700nm. The influence of roughness in the acoustic modes, in general, is relatively weak, and can be understood from the fact that they are composed of LA modes with long wavevectors [8, 10], which makes them very weakly affected by defects, and this is the case for both wider and ultra-narrow GNRs. Interestingly, a similar trend is observed for the optical modes (Fig. 2b) as well. For GNR widths W=5nm (red-dashed line) and W=3nm (green line), they indicate a semi-ballistic behavior even up to channel lengths of hundreds of nanometers. In the W=1nm and W=2nm cases, however, the optical modes reach the localization regime at lengths below L~100nm.

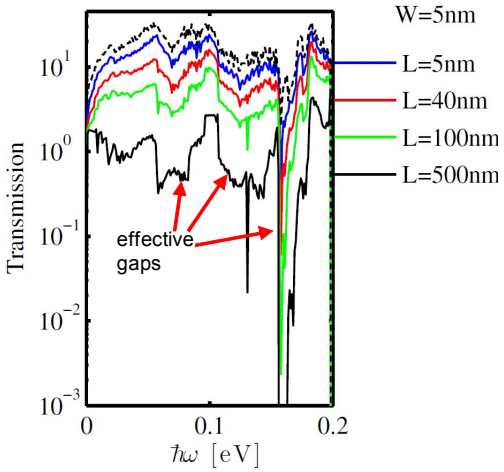

Fig. 3. The transmission function versus energy in logarithmic scale for rough edge GNRs of width W=5nm. The ballistic transmission (pristine GNRs, non-roughened ribbons) is depicted by the black-dashed line. Results for nanoribbons with lengths L=5nm (blue line), L=40nm (red line), L=100nm (green line), and L=500nm (black-solid line) are shown.

The behavior of the 'quasi-acoustic' modes (Fig. 2c), on the other hand, is very different. These modes enter the diffusive regime at much shorter channel lengths compared to the acoustic and the optical modes. They even enter the localization regime after L~300nm for the W=5nm GNRs, after L~100nm for the W=3nm GNRs, and just after L~10nm for the W=1nm GNRs. This is quite intriguing since these are dispersive modes with much higher group velocities compared to the optical modes. The strongest reduction in transmission, however, is observed for the energy regions E~0.16eV (Fig. 2d), which are regions of low mode density (see Fig. 1). For these modes, the transmission is diminished after channel lengths of L~200nm in the case of the wider channels, and after L~10nm in the case of the ultra-narrow channel.

The reason why the 'quasi-acoustic' mode regions and the low density mode regions behave so drastically different compared to the optical modes can be explained by their behavior under confinement. Figure 1 shows that under confinement, the number of modes in these energy regions (E~0.13, and E~0.16) is reduced significantly, making these regions look almost 'empty' of modes. In the presence of line edge roughness in a real geometry, the sparsity of the modes makes these particular energy regions more susceptible to the formation of 'effective' bandgaps by increasing the band mismatch between the modes in the physical channel regions along the propagation path of the phonons. Such an event is not the case for the optical modes for the geometries we examine. The 'effective' transmission bandgap formation is demonstrated in the transmission functions shown in logarithmic scale in Fig. 3 for the W=5nm channel under ballistic (pristine channel) conditions (black-dashed line) and under line edge roughness when the channel length is L=5nm, 40nm, 100nm, and 500nm (black-solid line). For short channels, the transmission is not significantly disturbed. For the longer channels, however, it is evident that for energies around E~0.07eV and E~0.13eV large 'effective' bandgaps form as indicated by the arrows. Notice the even larger

bandgap formation at energies E~0.16eV. Comparing this to Fig. 1b, there is a clear indication that the energy regions which become sparse of modes under confinement are very susceptible to roughness in less confined geometries as well. This suggests that the influence of confinement has similar features in the transmission as the effect of roughness.

The behavior described above should hold for any sparse mode energy regions. Note, for example, that gaps do not form in the regions of the 'flat' optical modes, and the transmission does not degrade as much. Under strong confinement, however, the 'flat' optical mode regions become sparser, and in extreme cases begin to 'look' like the low-density regions as well. Under these conditions, they could also be subject to band mismatch, and to the effect we describe above. In this context, the thermal conductivity is a function of the width-dependent phonon spectra **[15]**, for which line edge roughness could either further increase the band mismatch, or form 'effective' transport bandgaps.

An important message we convey in this work is the fact that just by looking at how the phonon bandstructure behaves under confinement, and its low-dimensional dispersion features, one can provide an indication of how the modes will behave under edge roughness. In addition, qualitatively, the behavior we describe should hold for other low-dimensional materials beyond GNRs, but also be relevant to phonon dispersions extracted through other methods, e.g. DFT calculations etc.

V. Conclusions

In conclusion, we have investigated the thermal transport properties of low-dimensional, ultra-narrow graphene nanoribbon (GNR) channels under the influence of line edge roughness disorder. We employed the non-equilibrium Green's function (NEGF) method for phonon transport and the force constant method for the description of the phonon modes. We show that the effect of line edge roughness affects different parts of the spectrum in different ways: i) Disorder does not affect the low frequency acoustic modes significantly, except under extreme confinement in purely 1D channels; ii) Disorder is not very detrimental for regions of the spectrum with a dense population of modes such as the optical modes as well; iii) Regions of the spectrum with low mode density end up becoming 'effective' transport gaps as the length of the channel increases, or the width decreases, and contribute little to thermal transport; iv) Regions of the spectrum with very low mode densities, populated with relatively 'flat' modes suffer from band mismatch in the presence of both confinement or roughness, which reduces their ability to carry heat. This drives transport at those energies into the localization regime.

Acknowledgment

The authors acknowledge Dr. Mahdi Pourfath, Dr. Hans Kosina, and Dr Mischa Thesberg for helpful discussions.

References

[1] N. Mingo, D. A. Broido, "Length dependence of carbon nanotube thermal conductivity and the "problem of long waves"," Nano Lett., 5, pp. 1221-1225, 2005.

[2] D. L. Nika, A. S. Askerov, and A. A. Balandin, "Anomalous size dependence of the thermal conductivity of graphene ribbons," Nano Lett., 12, pp. 3238-3244, 2012.

[3] L. Lindsay, D. A. Broido, and N. Mingo, "Lattice thermal conductivity of single-walled carbon nanotubes: Beyond the relaxation time approximation and phonon-phonon scattering selection rules," Phys. Rev. B, 80, 125407, 2009.

[4] L. Lindsay, D. A. Broido, and N. Mingo, "Flexural phonons and thermal transport in graphene," Phys. Rev. B, 82, 15427, 2010.

[5] D. L. Nika and A. A. Balandin, "Two-dimensional phonon transport in graphene," J. Phys.: Condens. Matter, 24, 233203, 2012.

[6] A. Balandin, "Thermal properties of graphene and nanostructured carbon materials," Nat. Materials,10, p. 569, 2011.

[7] A. V. Savin and Y. S. Kivshar "Vibrational Tamm states at the edges of graphene nanoribbons," Phys. Rev. B, 81, 165418, 2010.

[8] Z. Aksamija and I. Knezevic, "Lattice thermal transport in large-area polycrystalline graphene," Phys. Rev. B., 90, 035419, 2014.

[9] H. Karamitaheri, N. Neophytou, M. Pourfath, R. Faez, and H. Kosina, "Engineering Enhanced Thermoelectric Properties in Zigzag Graphene Nanoribbons," J. Appl. Phys., 111, 054501, 2012.

[10] Y. Wang, B. Qiu, and X. Ruan, "Edge effect on thermal transport in graphene nanoribbons: A phonon localization mechanism beyond edge roughness scattering," Appl. Phys. Lett., 101, 013101, 2012.

[11] F. Mazzamuto, J. Saint-Martin, A. Valentin, C. Chassat, and P. Dollfus, "Edge shape effect on vibrational modes in graphene nanoribbons: A numerical study," J Appl. Phys., 109, 064516, 2011.

[12] Z. W. Tan, J.-S. Wang, and C. K. Gan, "First-principles study of heat transport properties of graphene nanoribbons," Nano Lett., 11, pp. 214–219, 2011.

[13] D. Donadio and G. Galli, "Atomistic Simulations of Heat Transport in Silicon Nanowires," Phys. Rev. Lett. 102, 195901, 2009.

[14] M. Luisier, "Investigation of thermal transport degradation in rough Si nanowires," J. Appl. Phys., 110, p. 074510, 2011.

[15] W. J. Evans, L. Hu, and P. Keblinski, "Thermal conductivity of graphene ribbons from equilibrium molecular dynamics: Effect of ribbon width, edge roughness, and hydrogen termination," Appl. Phys. Lett., 96, 203112, 2010.

[16] A. Hochbaum, R. Chen, R. Delgado, W. Liang, E. Garnett, M. Najarian, A. Majumdar, and P. Yang, "Enhanced thermoelectric efficiency of rough silicon nanowires," Nature, 451, 163, 2008.

[17] A. I. Boukai, Y. Bunimovich, J. Tahir-Kheli, J.-K. Yu, W. A. Goddard, and J. R. Heath, "Silicon nanowires as efficient thermoelectric materials," Nature, vol. 451, pp. 168-171, 2008.

[18] T. Markussen, A.-P. Jauho, and M. Brandbyge, "Heat conductance is strongly anisotropic for pristine silicon nanowires," Nano Lett., 8, 3771, 2008.

[19] H. Karamitaheri, N. Neophytou, M. Pourfath, and H. Kosina, J. of Computational Electronics, "Study of Thermal Properties of Graphene-Based Structures Using the Force Constant Method," 11, 1, pp. 14-21, 2012.

[20] R. Saito, M. Dresselhaus, G. Dresselhaus, 'Physical Properties of Carbon Nanotubes', Imperial College Press, London, 1998.

[21] L. Lindsay, W. Li, J. Carrete, N. Mingo, D. A. Broido, and T. L. Reinecke, "Enhanced thermal conductivity and isotope effect in single-layer hexagonal boron nitride," Phys. Rev. B, 89, 155426, 2014.

[22] E. Pop, V. Varshney, and A. K. Roy, "Thermal properties of graphene: Fundamentals and applications," MRS Bulletin, 37, pp. 1273-1281, 2012.

[23] B. Vermeersch, A.M.S. Mohammed, G. Pernot, Y.-R. Koh, A. Shakouri, "Supperdiffusive heat conduction in semiconductor alloys," arXiv: 1406.7341, 2014.